Experimental Evaluation of the Impact of Body Obstruction on UWB Distance Estimation Accuracy: Comparative Analysis of Multiple Locations on the Human Body

Danny Daniel Díaz López
Universidad del Cauca
Popayán, Cauca, Colombia
danieldiaz@unicauca.edu.co

Victor Quintero
Universidad del Cauca
Popayán, Cauca, Colombia
vflorez@unicauca.edu.co

Abstract—**Ultra-Wideband (UWB) technology offers high accuracy in distance estimation, a crucial characteristic for localization and tracking systems. However, when people carry UWB devices, the accuracy of distance measurements can be compromised by signal absorption and blocking due to the human body, as well as by environmental propagation conditions. This work presents a comprehensive experimental evaluation of distance estimation accuracy, specifically analyzing the influence of device location on seven parts of the human body: head, hips, hands, wrists, chest, knees, and ankles, under different channel conditions: Line of Sight (LOS) and Non-Line of Sight (NLOS). The study employs DWM1001 UWB modules and the Two-Way Ranging (TWR) technique to obtain distance measurements in two representative scenarios: an outdoor environment (open space) and an indoor corridor. Key findings reveal that the chest location achieves the highest accuracy, with a Mean Absolute Error (MAE) of 0.0364 m under outdoor LOS conditions. In contrast, the knee location exhibits the worst performance, with errors up to 2.23 m under outdoor NLOS conditions. The study identifies a counterintuitive phenomenon where specific device locations, such as the hand and wrist, present superior performance under NLOS conditions compared to LOS in confined environments. The degradation factor ranges between 1.5× and 16.3× when transitioning from LOS to NLOS conditions, with an overall MAE of 0.3944 m for all configurations. The results provide a detailed characterization of how device location on the body and channel conditions affect UWB distance estimation accuracy, offering guidelines for the design and deployment of applications that require precise distance measurements with wearable devices.**

Keywords—**Ultra-Wideband (UWB), Distance Estimation Accuracy, Body Shadowing, LOS/NLOS Channel Conditions.**

I. INTRODUCTION

Precise Indoor Positioning Systems (IPS) have experienced exponential demand driven by the growth of Internet of Things (IoT) applications, indoor navigation, smart logistics, health monitoring, and immersive entertainment [1], [2]. Global Navigation Satellite Systems (GNSS) are ineffective in indoor scenarios due to severe signal attenuation from satellites [3]. This limitation has motivated the exploration of alternative technologies such as Wi-Fi, Bluetooth Low Energy (BLE), ultrasound, and UWB for positioning in these environments [4], [5]. UWB technology has emerged as the most promising solution for applications demanding high localization accuracy. Its superior capability derives from accurate measurement of the time of flight (ToF) of short-duration radio pulses, directly translating into accurate distance estimates between devices. Additionally, UWB presents robustness against multipath propagation and low energy consumption [5]–[8]. The Two-Way Ranging (TWR) technique constitutes the standard method employed by UWB devices for distance estimation, eliminating the need for synchronization between nodes [9], [10].

In practical applications, such as indoor navigation, industrial worker monitoring, patient tracking in hospitals, and location-based entertainment systems, UWB devices are typically carried by users. This configuration introduces critical technical challenges: the human body absorbs, reflects, and diffracts UWB signals, significantly altering signal intensity and arrival time [11]. This interaction generates body shadowing, creating Non-Line of Sight (NLOS) conditions between the mobile device and fixed reference nodes, consequently degrading distance estimation accuracy [2]. The scientific literature has addressed UWB channel modeling through statistical approaches [12]–[15], although these studies frequently omit body shadowing effects. Previous research has focused on body shadowing effects in conventional frequency bands [16], [17] or has developed statistical distance error models to mitigate the impact of the human body [18]. Otim et al. [19] analyzed NLOS conditions according to device position on the human body, concluding that body shadowing presents a greater impact when the device is located on the chest. However, comprehensive studies that systematically evaluate multiple body locations of the mobile device under different propagation conditions remain limited. The present work establishes its original contribution through systematic experimental evaluation of the impact of body shadowing

Parameter	Value	Unit
UWB Channel	5	–
Nominal Central Frequency	6489.6	MHz
Nominal Bandwidth	499.2	MHz
Data Transmission Rate	6.8	Mbps
Pulse Repetition Frequency (PRF)	64	MHz
Preamble Length	128	symbols
Preamble Code (TX/RX)	10	–
Transmission Power	-17	dBm
Receiver Sensitivity	-93	dBm

A. Indoor   B. Outdoors

Figure 1. Experimental scenarios. (A) Indoor: confined corridor. (B) Outdoor: open space.

on distance estimation accuracy in a 6.5 GHz UWB system. Specifically, this study analyzes seven distinct body locations of the mobile device, i.e., head, hips, hands, wrists, chest, knees, and ankles, under LOS and NLOS conditions in two representative scenarios. The main novelty lies in the comprehensive characterization of how different body locations of the mobile device affect measurement accuracy, providing for the first time a detailed comparative analysis that includes quantification of the degradation factor for each configuration. The specific objectives of the study include: (1) quantifying UWB distance estimation accuracy for each body location of the mobile device; (2) characterizing the impact of LOS/NLOS conditions on different locations; (3) identifying optimal body locations of the mobile device for specific applications; and (4) providing practical guidelines for the deployment of wearable UWB-based localization systems. This work is structured as follows: Section II describes the experimental methodology, including device configuration, test scenarios, and data collection procedures. Section III presents the experimental results, accompanied by a comprehensive statistical analysis. Section IV discusses the main findings and their implications. Finally, Section V presents the conclusions and future work.

II. METHODS

This section outlines the experimental methodology developed to assess the accuracy of straight-line distance estimation using UWB devices. The main methodological contribution consists of designing a systematic experimental protocol that enables the comprehensive characterization of the impact of body shadowing on multiple anatomical locations under controlled propagation conditions.

A. Device Configuration and System Parameters

The experiments employed the Qorvo DWM1001 development kit. Each module integrates a DW1000 UWB transceiver, a Nordic Semiconductor nRF52832 microcontroller, and a motion sensor [20]. The modules operated with Qorvo's PANS (*Positioning and Networking Stack*) firmware, implementing the TWR technique for distance estimation [8], [9]. The UWB device configuration was kept constant during all measurements to ensure result comparability, as presented in Table I. In the experimental configuration, one DWM1001 module functioned as a fixed reference node while another acted as a mobile device. The mobile device was sequentially placed
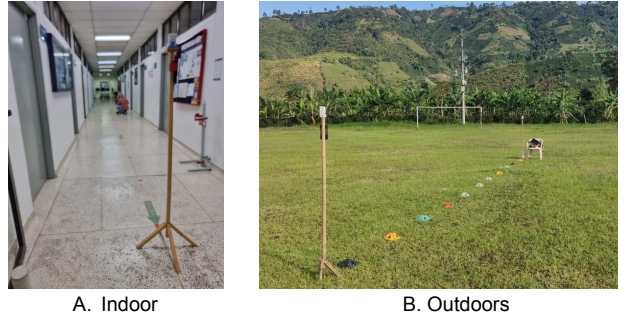
on different parts of the test subject's body, who moved over predefined distances. This configuration allowed the collection of multiple measurements for robust statistical analysis.

B. Experimental Scenario Design

The study implemented two main scenarios to evaluate different propagation conditions, as illustrated in Fig.1:

Outdoor Scenario: An open field with dimensions similar to a soccer field was used to have propagation conditions that minimize reflections from vertical structures, such as walls, thereby providing a baseline environment for analyzing primary propagation effects. This scenario enables the isolation of the impact of body shadowing on the direct signal while considering fundamental propagation phenomena, such as Free Space Path Loss (FSPL) and multipath generated by ground reflection.

Indoor Scenario: A corridor with approximate dimensions of 3 m wide by 20 m long was employed. This scenario introduces controlled multipath effects resulting from reflections off walls, the ceiling, and the floor, representing typical conditions in indoor applications.

In both scenarios, measurements were performed by systematically varying the distance between the fixed node and the mobile device in 1 m increments, covering a range from 1 m to 13 m, which is relevant for practical indoor localization applications.

C. Body Locations of the Mobile Device and Propagation Conditions

To comprehensively evaluate the impact of device location on the human body, the mobile UWB device was sequentially placed at seven anatomical positions on the test subject, as shown in Fig.2:

- **Head:** Device located on the upper cranial part
- **Hip:** Positioned laterally at belt level
- **Hand:** Held directly in the dominant hand
- **Wrist:** Worn as a wristband device
- **Chest:** Centered on the anterior torso (approximate height 1.5 m)
- **Knee:** Located on the frontal or lateral surface of the knee
- **Ankle:** Positioned on the external surface of the ankle
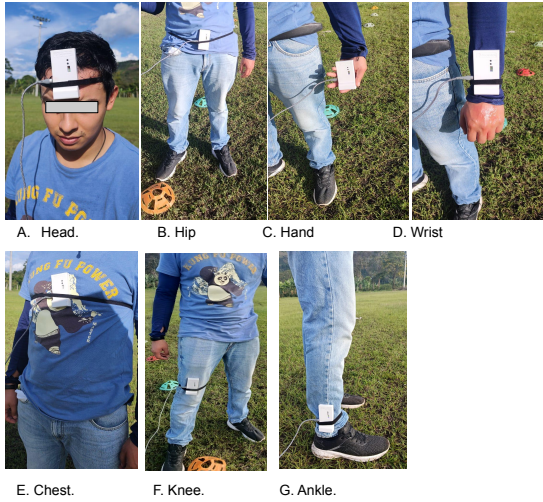
Figure 2. Mobile device locations on the body. A. Head. B. Hip. C. Hand. D. Wrist. E. Chest. F. Knee. G. Ankle.

For each body location of the mobile device and scenario, measurements were performed under two propagation conditions defined by the body orientation relative to the fixed node:

LOS Condition: A direct visual path between the fixed node and the mobile device was ensured. The subject was oriented so that the body part carrying the device maintained direct visibility with the reference node.

NLOS Condition: The direct line of sight between the fixed node and the mobile device was obstructed primarily by the human body. This condition was achieved by orienting the subject with their back to the fixed node, ensuring that the body part with the device blocked direct propagation. To ensure consistency across all NLOS measurements, the subject was instructed to maintain a standardized, upright posture, facing directly away from the fixed node, with arms resting naturally at their sides.

D. Data Collection Protocol

The experimental protocol followed the following systematized steps:

1) **Initial Setup:** The fixed node was positioned at the standard height of 1.5 m on a tripod. The mobile device was attached to the corresponding body location.

2) **Reference Distance Establishment:** For each combination of scenario, body location of the mobile device, and channel condition, the subject was positioned at predefined distances in a straight line relative to the fixed node. Real distances were accurately marked using measuring tape, starting from 1 m in unit increments.

3) **UWB Data Acquisition:** 250 estimated distance readings per measurement point were collected to ensure robust statistical analysis.

4) **Systematic Recording:** Real distance, estimated distance, body location of the mobile device, LOS/NLOS condition, and scenario were documented for each measurement. Subject orientation was kept consistent for each propagation condition.

E. Evaluation Metric and Statistical Analysis

The main metric for evaluating performance was distance estimation accuracy, quantified through the absolute distance error (e_d):

$$e_d = |d_{\text{estimated}} - d_{\text{real}}|, \tag{1}$$

where $d_{\text{estimated}}$ represents the distance measured by the UWB system and d_{real} corresponds to the physically measured distance.

From the set of error measurements for each configuration, a comprehensive statistical analysis was performed, including the calculation of mean absolute error (MAE), standard deviation, maximum error, and minimum error. These analyses allowed quantitative comparison of the impact of different variables on distance estimation performance.

Fig. 3 presents a consolidated analysis of the distance measurements, where each horizontal row corresponds to a unique experimental condition (combining environment, body part, and line of sight). The horizontal axis quantifies the estimated distance in meters. Along each row, the different colored clusters represent the 250 distance samples taken at each actual measurement point. Thus, the graph allows for a direct visual assessment of the accuracy and precision of the UWB system under each of the 28 configurations analyzed. The interpretation of the graph is intuitive: the concentration of the data points is directly proportional to the measurement's precision. When the points of a specific color are tightly clustered, as seen in the Outdoors CHEST LOS condition, it indicates high accuracy and precision. Conversely, a wide dispersion of points, as is evident in Outdoors KNEE NLOS, reflects low precision and high variability. This is a direct consequence of the adverse effect of body shadowing (NLOS) in an environment without reflections to aid the signal. This visualization not only quantitatively confirms the study's findings but also provides powerful qualitative insight into how the device's location on the body and environmental conditions drastically impact the reliability of distance estimation.
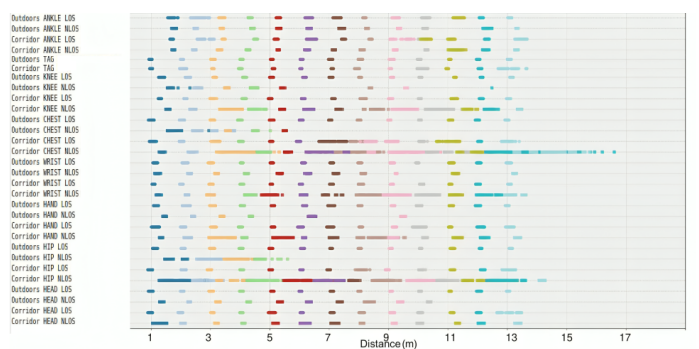

Figure 3. Distribution of UWB distance estimations across all experimental configurations. The vertical axis details each of the 28 test conditions, combining the scenario (Outdoor/Indoor), the on-body device location, and the line-of-sight condition (LOS/NLOS). Each colored cluster of points along a horizontal row represents the 250 measurements recorded at a specific ground-truth distance, visually displaying the system's accuracy and precision (clustering).

Table II
ACCURACY AND PRECISION IN OUTDOOR SCENARIO - LOS.

Location	MAE (m)	σ (m)
chest	0.0364	0.0309
head	0.0464	0.0283
wrist	0.0720	0.0571
hip	0.0817	0.0415
knee	0.1513	0.0877
ankle	0.3274	0.1554
hand	0.3672	0.4207

Figure 4. Statistical distribution of errors by scenario and line of sight condition. (a) Error distribution by scenario. (b) Density analysis.

III. RESULTS

This section presents the experimental results of the distance estimation accuracy evaluation using UWB devices, considering the impact of device location on the human body and LOS/NLOS propagation conditions in outdoor and indoor scenarios. The analysis employs the degradation factor (Nx) to numerically quantify the accuracy degradation when the human body obstructs the signal, calculated as the ratio between MAE in NLOS conditions and MAE in LOS conditions.

A. Global Analysis of UWB Distance Estimation Error

The experiments yielded substantial variations in distance estimation accuracy, depending on the experimental configuration. The analysis of 28 different configurations, i.e., 7 body locations of the mobile device × 2 LOS/NLOS conditions × 2 scenarios, produced the following global performance results:

- **Global Mean Absolute Error (MAE):** 0.3944 m
- **Root Mean Square Error (RMSE):** 0.6690 m
- **95th Percentile:** 1.1424 m

The 95th percentile indicates that 95% of all measurements present errors below 1.1424 m, providing a measure of the system's extreme variability. A consistent finding across all evaluated configurations was the systematic tendency to estimate distances greater than real ones, a phenomenon attributable to multipath and signal processing times in UWB devices. The probabilistic distribution of errors showed positive asymmetry with a tail of larger errors, indicating the non-Gaussian nature of errors in specific configurations, particularly under NLOS conditions.

B. Performance Characterization by Body Location of the Mobile Device

1) Outdoor Scenario - LOS Conditions: In the outdoor scenario under LOS conditions, locations on the upper and central part of the torso presented the highest accuracy. Table II presents the detailed performance. Upper locations (chest and head) are characterized by a lower degree of obstruction, resulting in higher accuracy in distance estimation. The chest location achieved the lowest recorded mean absolute error, i.e., MAE = 0.0364 m. At the same time, the hand exhibited the highest standard deviation and relative variability, i.e., σ = 0.4207 m and coefficient of variation CV = 114.6%.
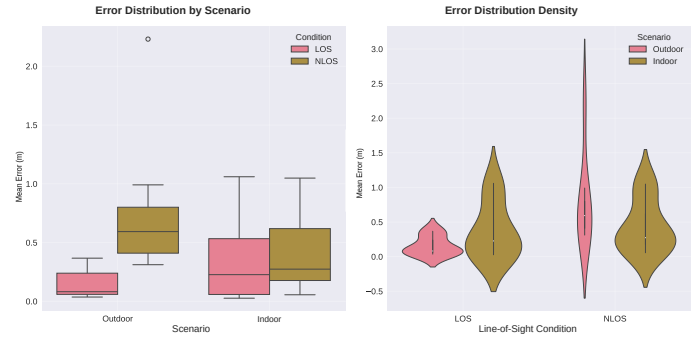
2) Outdoor Scenario - NLOS Conditions: The transition from LOS to NLOS conditions induced significant degradations in distance estimation accuracy for all evaluated locations. The most notable case was the chest location, where the error increased from 0.0364 m to 0.5932 m, representing a degradation factor of 16.3×. The highest variability behavior was recorded at the knee, with a mean error of 2.2312 ± 1.7962 m and a maximum error value of 5.48 m, constituting the worst scenario identified in the study.

3) Indoor Scenario - LOS Conditions: The indoor scenario introduces additional complexities that significantly alter performance. Under LOS conditions, very high accuracy was observed, even surpassing the outdoor scenario in some cases. The chest location achieved the lowest mean absolute error, i.e., MAE = 0.0266 m, establishing itself as the most accurate position for this scenario. In contrast, the wrist location showed significantly degraded performance with an MAE of 1.0599 m, indicating that this body position is particularly problematic in confined environments under LOS conditions.

4) Indoor Scenario - NLOS Conditions: Contrary to conventional theoretical predictions, some body locations of the mobile device exhibited better performance in NLOS conditions than in LOS, as presented in the following MAE:

- Hand: LOS 0.9020 m vs NLOS 0.2471 m (factor 0.36×)
- Wrist: LOS 1.0599 m vs NLOS 0.1777 m (factor 0.60×)
- Ankle: marginal improvement (factor 0.9×)

This behavior suggests that the presence of reflective surfaces in the confined scenario can generate multipath propagation conditions that, under specific body orientations, can result in more accurate estimates than obstructed direct propagation. Fig.4 shows the statistical distribution of errors by scenario and line of sight condition. The box plot (left) indicates that the indoor scenario exhibits a slightly lower median error in LOS conditions compared to outdoor conditions. Greater variability is observed in the outdoor scenario for NLOS conditions, as indicated by the extended whiskers and the presence of outliers. The density analysis (right) confirms the non-Gaussian nature of errors, showing asymmetric distributions with extended tails toward larger errors, particularly in NLOS conditions. Fig.5 shows the LOS vs NLOS comparison by body location of the mobile device. The head and chest locations exhibit behaviors relatively consistent with traditional theory,
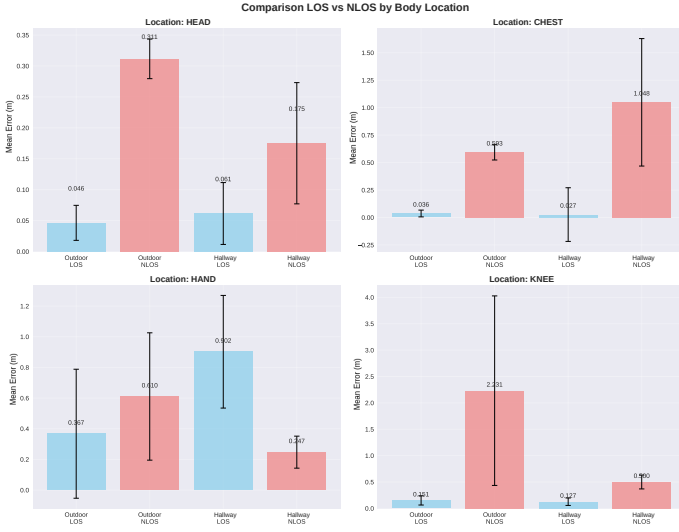
Figure 5. Detailed LOS vs NLOS comparison by body location of the mobile device.


Figure 6. System variability and stability. (a) Scatter plot showing the relationship between mean error and standard deviation. (b) Coefficient of variation by body location of the mobile device presents the relative stability of each configuration

where LOS conditions (blue bars) generally result in lower errors than NLOS (red bars), although the chest experiences particularly severe degradation in NLOS conditions within the indoor scenario. However, the hand and knee locations reveal the phenomenon where specific configurations show superior performance in NLOS conditions compared to LOS in the indoor scenario. This behavior can be explained by body orientation in confined spaces, where specular reflections from the walls of the indoor scenario may provide more favorable propagation paths than the direct signal, which is obstructed by the body. Fig. 6 shows the standard deviation and coefficient of variability of distance estimation in the different configurations. The scatter plot (upper) reveals three distinct behavioral regions: a high-performance zone (lower left corner) where optimal configurations with low error and low variability are concentrated; an intermediate region with moderate performance; and a problematic zone (upper right corner) dominated by knee in NLOS condition that exhibits high MAE, i.e., 2.2 m and high variability, i.e., $\sigma = 1.8$ m.

IV. DISCUSSION

The analysis of the outdoor scenario, while intended as a baseline, reveals complex interactions that go beyond simple line-of-sight propagation. Although this environment was free from wall reflections, the results must be interpreted in the context of fundamental radio propagation models. The Free Space Path Loss (FSPL) model provides a theoretical benchmark for signal attenuation; however, our experimental results show deviations that can be attributed to several factors. Firstly, the ground surface acts as a significant reflector, creating a two-ray multipath condition. This can result in either constructive or destructive interference at the receiver, contributing to the variability and error observed even in LOS conditions. Secondly, the human body itself acts as a dynamic component of the antenna system. The placement and orientation of the UWB device on different body parts
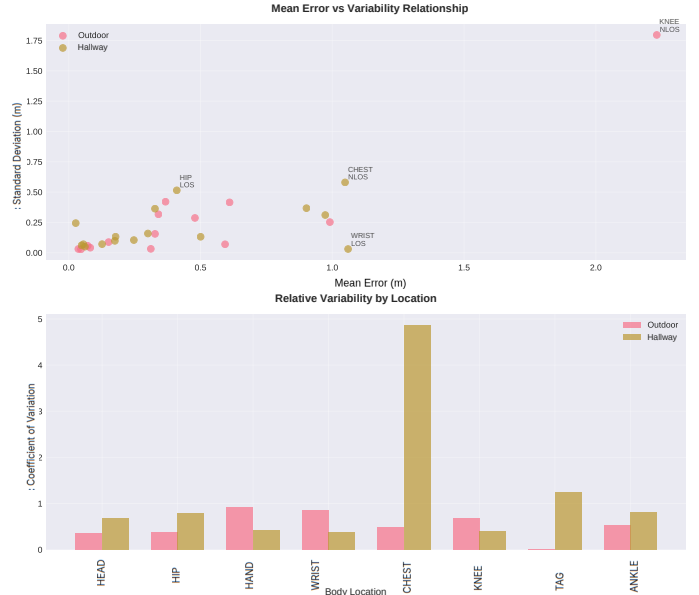
inherently alter the antenna's effective radiation pattern. As discussed by Zekavat [3], [21], antenna polarization and orientation are critical. For instance, the orientation of the device on the hand or ankle can cause the main lobe of the radiation pattern to focus away from the receiver, resulting in higher-than-expected signal attenuation and thus degrading accuracy. This highlights that even in an open field, the propagation environment is far from simple, a complexity also noted in the survey by Alarifi et al [5]. Therefore, the outdoor results provide critical insight into how the body perturbs the radiation field even in the absence of environmental clutter. The most significant finding is the identification of configurations where specific body locations of the mobile device, i.e., the wrist and hand, exhibit better performance in NLOS conditions compared to LOS in confined environments. This phenomenon can be explained through several physical mechanisms. When the subject is oriented with their back to the fixed node in the indoor scenario, the device antenna is positioned laterally relative to the body, potentially minimizing direct obstruction. Simultaneously, specular reflections from corridor walls act as a waveguide, providing alternative propagation paths that can be more favorable than the obstructed direct signal. Statistical analysis confirms the non-Gaussian distribution of errors, with a systematic tendency toward distance overestimation, i.e., global mean error of 0.3944 m. This characterization suggests that traditional error models based on Gaussian distributions may be inadequate for characterizing the behavior of UWB systems with body shadowing. Performance variability between body locations of the mobile device reaches degradation factors of up to 16.3x, highlighting the critical importance of selecting an appropriate location for specific applications. For indoor navigation applications requiring high accuracy,

chest and head locations emerge as optimal options under LOS conditions. For continuous monitoring applications where NLOS conditions are frequent, wrist and hand locations may offer more robust performance in confined environments. These findings have significant implications for the design of localization algorithms. Adaptive systems that identify and leverage constructive multipath conditions could significantly improve accuracy in indoor environments. Additionally, the results suggest the need for LOS/NLOS classification algorithms specific to different body locations of the mobile device.

V. Conclusions

This work presented a comprehensive experimental evaluation of distance estimation accuracy using UWB devices, focusing on the impact of mobile device location on seven body locations of the mobile device, i.e., head, hip, hand, wrist, chest, knee, and ankle, and LOS/NLOS propagation conditions in two representative scenarios. The results showed that the location of the UWB device on the human body critically impacts accuracy. The chest achieved the highest accuracy, i.e., MAE = 0.0364 m, under outdoor LOS conditions, while the knee exhibited the worst performance, i.e., up to 2.23 m under outdoor NLOS conditions. Degradation factors varied from 1.5 times to 16.3 times, indicating the critical importance of selecting an appropriate body location for the mobile device.

A phenomenon was identified where locations such as the hand and wrist showed better performance under NLOS conditions than LOS in indoor environments, suggesting that specific multipath configurations in confined spaces can be beneficial for distance estimation.

The global mean absolute error of 0.3944 m and the non-Gaussian distribution of errors provide fundamental statistical characterization for the design of wearable UWB-based localization systems. The findings provide practical guidelines for specific applications, including chest and head locations for maximum accuracy in LOS conditions, and wrist and hand locations for robustness in confined environments with frequent body shadowing.

It is essential to acknowledge that this work was conducted as a foundational case study with a single test subject. This approach allowed for a detailed characterization of device location and channel effects by minimizing inter-subject variability. However, to ensure the generalization of these findings for robust wearable applications, future work must focus on an exhaustive test plan involving multiple subjects with diverse bodily conditions and anthropometric characteristics, i.e., height, weight, and Body Mass Index (BMI). Furthermore, future work will also include evaluating adaptive algorithms that leverage constructive multipath conditions, as well as developing statistical models tailored to different body locations of the mobile device, to enhance the accuracy of UWB localization systems in real-world applications.

VI. Acknowledgements

References

[1] Koyuncu H, Yang h. A survey of indoor positioning and object locating systems. IJCSNS International Journal of Computer Science and Network Security. 2010 May;10(5):121–128.

[2] Zafari F, Gkelias A, Leung KK. A survey of indoor localization systems and technologies. IEEE Communications Surveys Tutorials. 2019; 21(3):2568–2599.

[3] Zekavat SA. An introduction to the fundamentals and implementation of wireless local positioning systems. In: Handbook of position location. IEEE Press; 2011. p. 1169–1194.

[4] Al-Ammar MA, Alhadhrami S, Al-Salman A, et al. Comparative survey of indoor positioning technologies, techniques, and algorithms. In: Proc. International Conference on Cyberworlds; 2014. p. 245–252.

[5] Alarifi A, Al-Salman AM, Alsaleh M, et al. Ultra wideband indoor positioning technologies: Analysis and recent advances. Sensors. 2016 May;16(5):1–36.

[6] Wang N, Yuan X, Ma L, et al. Research on indoor positioning technology based on UWB. In: Proc. Chinese Control And Decision Conference (CCDC); 2020. p. 2317–2322.

[7] Mainetti L, Patrono L, Sergi I. A survey on indoor positioning systems. In: Proc. 22nd International Conference on Software, Telecommunications and Computer Networks (SoftCOM); 2014. p. 111–120.

[8] Ridolfi M, Van de Velde S, Steendam H, et al. Analysis of the scalability of UWB indoor localization solutions for high user densities. Sensors. 2018 Jun;18(6):1–19.

[9] An JH, Choi L. Inverse fingerprinting: Server side indoor localization with Bluetooth low energy. In: Proc. IEEE 27th Annual International Symposium on Personal, Indoor, and Mobile Radio Communications (PIMRC); 2016. p. 1–6.

[10] Mikhaylov K, Petäjäjärvi J, Hämäläinen M, et al. Impact of IEEE 802.15.4 communication settings on performance in asynchronous two way UWB ranging. International Journal of Wireless Information Networks. 2017;24(2):124–139.

[11] Otim T, Díez LE, Bahillo A, et al. Effects of the body wearable sensor position on the UWB localization accuracy. Electronics. 2019 Nov; 8(11):1–14.

[12] Ramirez-Mireles F. On the performance of ultra-wide-band signals in Gaussian noise and dense multipath. IEEE Transactions on Vehicular Technology. 2001 Jan;50(1):244–249.

[13] Fiorina J, Domenicali D. The non validity of the Gaussian approximation for multi-user interference in ultra wide band impulse radio: From an inconvenience to an advantage. IEEE Transactions on Wireless Communications. 2009 Nov;8(11):5483–5489.

[14] Beaulieu NC, Niranjayan S. UWB receiver designs based on a Gaussian–Laplacian noise-plus-MAI model. IEEE Transactions on Communications. 2010 Mar;58(3):997–1006.

[15] Ahmed QZ, Park KH, Alouini MS. Ultrawide bandwidth receiver based on a multivariate generalized Gaussian distribution. IEEE Transactions on Wireless Communications. 2015 Apr;14(4):1800–1810.

[16] Blas J, Lago FA, Fernández P, et al. Potential exposure assessment errors associated with body-Worn RF dosimeters. Bioelectromagnetics. 2007 Oct;28(7):573–576.

[17] Ambroziak SJ, et al. An off-body channel model for body area networks in indoor environments. IEEE Transactions on Antennas and Propagation. 2016 Sep;64(9):4022–4035.

[18] Cully WPL, Cotton SL, Scanlon WG, et al. Body shadowing mitigation using differentiated LOS/NLOS channel models for RSSI-based Monte Carlo personnel localization. In: Proceedings of the IEEE Wireless Communications and Networking Conference (WCNC); Apr; 2012. p. 694–698.

[19] Otim T, Bahillo A, Díez LE, et al. Impact of body wearable sensor positions on UWB ranging. IEEE Sensors Journal. 2019 Dec;19(23):11449–11457.

[20] Qorvo. DWM1001 datasheet [https://www.qorvo.com/products/d/da007950]; 2017. [Accessed: 24-Jul-2022].

[21] Zekavat R, Buehrer RM. Wireless positioning systems: operation, application, and comparison. In: Handbook of position location: Theory, practice, and advances. IEEE; 2019. p. 3–23.